Eur. Phys. J. Special Topics **222**, 861–873 (2013)

DOI: 10.1140/epjst/e2013-01889-8

THE EUROPEAN PHYSICAL JOURNAL SPECIAL TOPICS

Regular Article

How do global temperature drivers influence each other?

A network perspective using recurrences

Bedartha Goswami[1,2,a,b], Norbert Marwan[1], Georg Feulner[1], and Jürgen Kurths[1,3,4]

[1] Potsdam Institute for Climate Impact Research, 14412 Potsdam, Germany
[2] Department of Physics, University of Potsdam, 14476 Potsdam, Germany
[3] Department of Physics, Humboldt University Berlin, 12489 Berlin, Germany
[4] Institute for Complex Systems and Mathematical Biology, University of Aberdeen, AB24 3UE Aberdeen, UK

Received 22 March 2013 / Received in final form 3 May 2013
Published online 11 July 2013

Abstract. We investigate a network of influences connected to global mean temperature. Considering various climatic factors known to influence global mean temperature, we evaluate not only the impacts of these factors on temperature but also the directed dependencies among the factors themselves. Based on an existing recurrence-based connectivity measure, we propose a new and more general measure that quantifies the level of dependence between two time series based on joint recurrences at a chosen time delay. The measures estimated in the analysis are tested for statistical significance using twin surrogates. We find, in accordance with earlier studies, the major drivers for global mean temperature to be greenhouse gases, ENSO, volcanic activity, and solar irradiance. We further uncover a feedback between temperature and ENSO. Our results demonstrate the need to involve multiple, delayed interactions within the drivers of temperature in order to develop a more thorough picture of global temperature variations.

1 Introduction

Global mean temperature is one of the primary quantities used to characterize Earth's climate and modern climate change. It has been, and still is, a central variable of interest in the research focussed on understanding global climate variability. In their fourth Assessment Report, the IPCC clarified to a large extent the role of anthropogenic forcings in the warming trend of the Global Mean Temperature (GMT) of the last century [1]. Although warming by anthropogenic greenhouse gases dominates the observed rise in temperature, uncertainties continue to persist in answers to questions such as: *how much* of the temperature change is induced *by which factors*, and *how*

[a] e-mail: goswami@pik-potsdam.de
[b] Former affiliation: Indian Institute of Science Education and Research, Pune 411021, India.

do they change the temperature. These questions interweave two crucial strands of GMT studies: (i) efforts to understand GMT variations of the past, and (ii) efforts to foresee how the climate (and not just the temperature) is going to change in the next decades. For the twentieth century, an increasing number of observational records of temperature have enabled us to move towards more comprehensive estimates of global temperature (cf. Sect. 3.2 of [2], and [3]). Despite having been able to narrow down the main suspects behind variations in global temperatures to anthropogenic influences, the El Niño Southern Oscillation (ENSO), volcanic activity, solar radiation, and internal climate variability, there still exists significant debate over the nature of the temperature response to climate change as shown by the diverse explanations put forth to explain the apparent recent "deceleration" of global warming [4]. In this context, studies such as that of Lean & Rind [5,6], and Foster & Rahmstorf [7] shed light on how the different factors affect global mean temperatures. Based on empirical multivariate regression models, Lean & Rind estimate the response of GMT to human activity, ENSO, volcanoes and changes in solar activity, and thereafter apply it to forecast (by various conditions) the global temperature for the next decade. The latter study of Foster & Rahmstorf presents a robust analysis to estimate the residual anthropogenic impact on the warming trend of the last three decades after removing the natural forcings to global temperature.

These studies, however, presuppose two things: (i) independence *between* the factors that impact temperature, and (ii) a linear superposition of their effects on temperature variations. Although it might be the case that both assumptions are valid to a fair (and practical) degree of approximation, it is critical to assess their validity scientifically.

The primary focus of this study is to address the first of the above assumptions and examine the manner in which, and if at all, the factors influencing global temperature interact among themselves. We use an empirical approach based on the recurrences of dynamical systems for this purpose. Recent developments in the theory of recurrences, and recurrence plots in particular, have made it an increasingly popular tool for scientific investigations (cf. [8] for a historical overview). Recurrence-based analysis has found application in a wide range of scenarios ranging from analyses of cardiac data [9] to stock markets [10] to cover song identification [11] to speech comprehension [12]. In the context of climate analyses, cross recurrence plots (CRPs) have been used to study links between ENSO and north-western Argentinian precipitation both in modern and "paleo" time scales [13]; and more recently, joint recurrence plots (JRPs) have been used to investigate the spatial distribution of links between vegetation and climatic variables such as temperature and precipitation [14].

We extend the idea behind the measure for lag/generalized synchronization put forth in [15]. The measure is based on JRPs and is suitable thus for the analysis of structurally different systems as in our case. We allow for delayed interactions up to delays of around 12 years among all considered datasets and test all estimated values for statistical significance – choosing only the statistically significant values for interpretations. The results presented here are an attempt to visualize a network of influences that are relevant to understanding GMT. They are intended to corroborate some of the existing ideas of links between climatic variables and GMT, as well as uncover new interactions among several of the impacting variables themselves.

The paper is organised as follows: In Sect. 2 we present the datasets used in this study. Section 3 reviews the theory underlying the recurrence-based connectivity measure, and Sect. 4 outlines the manner of significance tests used in the analysis. In Sect. 5, we detail the various steps involved in the analysis. Section 6 presents the results and their interpretation, and Sect. 7 provides a brief summary and outlook. Finally, the appendix provides the various sources of the datasets.

2 Data

Following Lean & Rind [5], we consider four critical contenders that have the potential to influence global mean temperature: (i) the ENSO, (ii) volcanic activity, (iii) solar irradiance, and (iv) the concentration of well-mixed greenhouse gases in the atmosphere. To characterise these phenomena, we choose: a combination of the multivariate El Niño index [16] (which extends from 1950 till present) and the index of Meyers et al. [17] (for data prior to 1950) for the ENSO; stratospheric aerosol optical thickness measurements compiled by Sato et al. [18] for volcanic activity; Wang et al.'s [19] reconstruction of total solar irradiance that extends to around 300 years back; annual global mean forcing values used for well-mixed greenhouse gases as used in the NASA GISS modelE [20] which were then interpolated to a monthly resolution. For the global temperature itself, we use two datasets: the NASA GISS Land-Ocean Temperature Index (LOTI) [3], and the surface temperature record HadCRUT3v assimilated by the Climate Research Unit (CRU) at East Anglia University [21]. (The source of the datasets are listed in Appendix A). We consider the 120 year period from January 1890 to December 2009 in which all the datasets are resolved on a monthly basis for the purpose of this study. Moreover, for the TSI dataset, we use a low pass filter using a Gaussian kernel of bandwidth $\approx$ 11 years, and we consider the first derivative of WMGHG instead of the almost monotonically increasing raw dataset (figure not shown). Note that, in contrast to Lean & Rind [5], we do not use the full anthropogenic forcing but just the well-mixed greenhouse gases. The final time series used in the analysis (normalized to mean zero and variance one) are shown in Fig. 1. For brevity, we henceforth refer to the datasets using the following labels: *CRUTA* for the HadCRUT3v data; *GISS* for NASA GISS LOTI; *TSI* for total solar irradiance; *VOLC* for the optical aerosol depth data; and *WMGHG* for the well-mixed greenhouse gas series.

3 Lagged dependencies using recurrences

Recurrence is a fundamental characteristic of dynamical systems that provide insight into their dynamical properties [22]. Defined as the return of the phase space trajectory of the system to an earlier state (up to a tiny deviation), in practice, recurrences are approximated as the return of the system to the *neighbourhood* of a previous state. If we consider a system X such that $\mathcal{X}$ is the set of all possible trajectories of X, a recurrence matrix $\mathbf{R}^X$ for a given trajectory $\mathbf{x} = \{\mathbf{x}_1, \mathbf{x}_2, \ldots, \mathbf{x}_N\} \in \mathcal{X}$ is defined as:

$$\mathbf{R}^X_{i,j}(\varepsilon) = \Theta(\varepsilon - \| \mathbf{x}_i - \mathbf{x}_j \|), \quad i, j = 1, \ldots, N. \tag{1}$$

Here, N is the trajectory length, ε the size of the neighbourhood, $\Theta(\cdot)$ the Heaviside function (i.e., $\Theta(\cdot) = 1$ for non-negative values and 0 otherwise) and $\| \cdot \|$ denotes an appropriate metric that quantifies 'distance'. A *recurrence plot* (RP) is a visual representation of $\mathbf{R}$ typically constructed by putting a black marker for every 1 in $\mathbf{R}$ (cf. [23] for a more detailed treatment of recurrence plots).

If we take any arbitrary trajectory $\mathbf{x}' \in \mathcal{X}$, the probability $P(\mathbf{x}' \sim \mathbf{x}_i)$ that a point $\mathbf{x}'_\mathbf{i} \in \mathbf{x}'$ visits the neighbourhood of $\mathbf{x}_i \in \mathbf{x}$ is equal to the column-sum of the recurrence matrix $\mathbf{R}^X$ (from Eq. (1)),

$$P(\mathbf{x}_i) = \frac{1}{N} \sum_{j=1}^{N} \mathbf{R}^X_{i,j}. \tag{2}$$

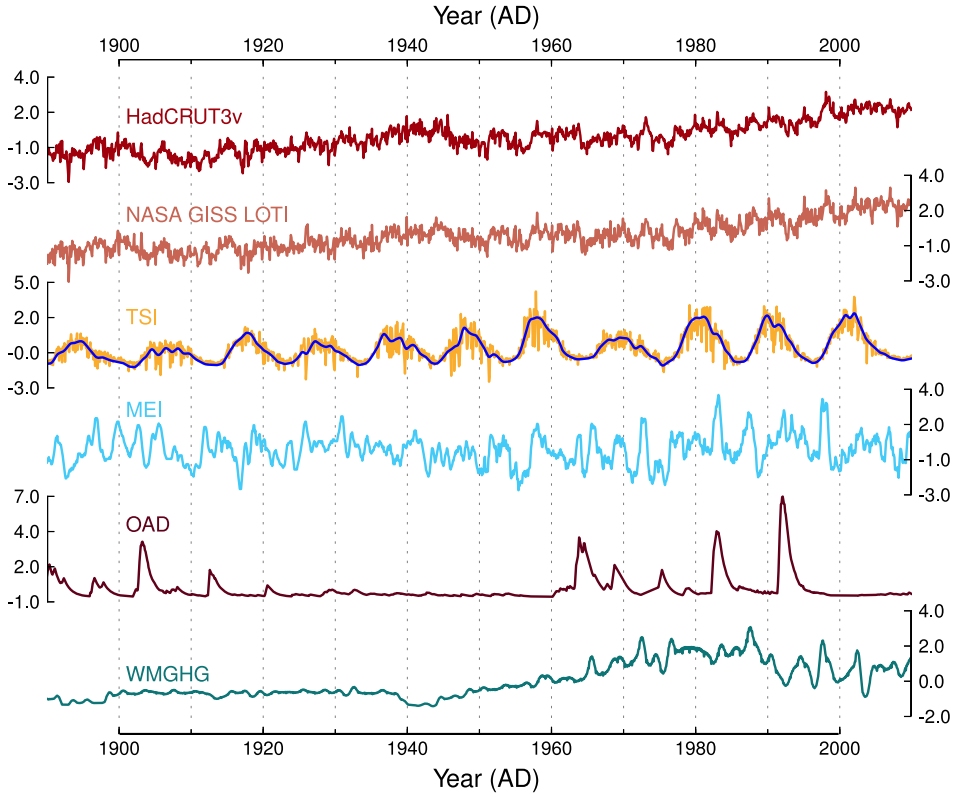

Fig. 1. Data used. From top to bottom: global surface temperature from the CRU at East Anglie (HadCRUT3v, **deep red**); NASA GISS Land-Ocean Temperature Index (NASA GISS LOTI, **light red**); Wang et al.'s reconstruction of total solar irradiance (TSI, **deep yellow**) with the Gaussian-kernel (bandwidth of ≈ 11 years) filtered curve (in **blue**); the Multivariate ENSO Index (MEI, **light blue**); Sato et al's volcanic activity index based on Optical Aerosol Depth (OAD, **brown**); monthly changes in the NASA GISS's modelE global mean forcing values for Well-Mixed GreenHouse Gases (WMGHG, **teal**).

where $P(\mathbf{x}_i)$ denotes $P(\mathbf{x}' \sim \mathbf{x}_i)$. The average probability of any trajectory of the system to recur to any given state is the mean $\langle P(\mathbf{x}_i) \rangle = \sum_{i=1}^{N} P(\mathbf{x}_i)/N$, and is known as the (global) *recurrence rate* (RR^X) of X.

In this study, we compare the recurrence structures of characteristically different systems in order to infer the influences that they might have on each other. A comparison of recurrence structures of two different systems can be performed using joint recurrences, and the corresponding joint recurrence matrix, defined as:

$$\mathbf{JR}_{i,j}^{XY}(\varepsilon_x, \varepsilon_y) = \Theta(\varepsilon_x - \| \mathbf{x}_i - \mathbf{x}_j \|) \, \Theta(\varepsilon_y - \| \mathbf{y}_i - \mathbf{y}_j \|) \quad i,j = 1, \ldots, N, \qquad (3)$$

where $\mathbf{x}$ and $\mathbf{y}$ are two given trajectories of systems X and Y respectively. A non-zero value $\mathbf{JR}_{i,j}^{XY}$ thus captures co-occurring recurrences of trajectories $\mathbf{x} \in \mathcal{X}$ and $\mathbf{y} \in \mathcal{Y}$ in corresponding neighbourhoods of systems X and Y respectively, i.e., $\mathbf{x_i} \sim \mathbf{x_j}$ and $\mathbf{y_i} \sim \mathbf{y_j}$ at the same time instant i (or j). Using $\mathbf{JR}^{XY}$, we now consider the joint probability that two arbitrary trajectories $\mathbf{x}' \in \mathcal{X}$ and $\mathbf{y}' \in \mathcal{Y}$ recur in the

neighbourhood of $\mathbf{x_i}$ and $\mathbf{y_i}$ simultaneously,

$$P(\mathbf{x}_i, \mathbf{y}_i) = \frac{1}{N} \sum_{j=1}^{N} \mathbf{JR}_{i,j}^{XY}, \tag{4}$$

where $P(\mathbf{x}_i, \mathbf{y}_i)$ denotes (as previously) the probability $P(\mathbf{x}' \sim \mathbf{x}_i, \mathbf{y}' \sim \mathbf{y}_i)$.

Previously, joint recurrences have been used to detect generalized synchronization (GS) as well as lag synchronization (LS) [15]. In their approach, the authors use the results that, (i) a topological reconstruction of the phase space trajectory is possible from a given recurrence matrix, and (ii) two systems governed by a functional relationship will have similar recurrence matrices. Furthermore, if two systems X and Y are in GS, their respective global recurrence rates $\langle P(\mathbf{x}_i) \rangle$ and $\langle P(\mathbf{y}_i) \rangle$ are approximately equal to the joint recurrence rate $\langle P(\mathbf{x}_i, \mathbf{y}_i) \rangle$. They suggest to use a *fixed number of nearest neighbours* as a threshold for the computation for the recurrence matrices such that $P(\mathbf{x}_i) = n_0/N \; \forall \; i$ where n_0 is the predefined number of nearest neighbours (the same number is used for system Y as well). In this case, the recurrence rates of X and Y are thus set to be equal, i.e., $\langle P(\mathbf{x}_i) \rangle = \langle P(\mathbf{y}_i) \rangle = n_0/N$. The measure for synchronization is then given by,

$$JPR = \max_{\tau} \frac{S(\tau) - R_0}{1 - R_0}, \tag{5}$$

where $R_0 = n_0/N$ and

$$S(\tau) = \frac{\langle P(\mathbf{x}_i, \mathbf{y} - i(\tau) \rangle}{R_0}. \tag{6}$$

In this study, we extend this idea to allow for the more general case where the two systems X and Y may have differing overall recurrent rates as well as the case where $P(\mathbf{x}_i) \neq P(\mathbf{y}_i)$. In particular, in order to estimate how 'non-independent' X and Y are from each other, we are interested in the quantity,

$$RMD_i = \frac{P(\mathbf{x}_i, \mathbf{y}_i)}{P(\mathbf{x}_i) P(\mathbf{y}_i)}. \tag{7}$$

Here, RMD denotes *Recurrence-based Measure of Dependence*. (We note that such a probabilistic ratio is already a quantity of interest in medical analysis and is termed as the "*Odds-to-Expected ratio*", or the O/E ratio in short [29].) However, we wish to quantify the direction of dependency between X and Y as well. RMD_i, as defined above, is symmetric for X and Y and cannot detect the direction of influence. Other recurrence-based methods, such as that of the *Mean Conditional Probability of Recurrence* (MCR) [24–26], help to infer the direction of coupling between a pair of datasets but it is non-trivial to extend the notion of MCR for delayed couplings. We argue that, similar to $S(\tau)$ (Eq. (6)), it is natural to incorporate lagged probabilities in RMD_i simply by introducing a relevant lag in one of the systems. We thus define the log-mean $RMD(\tau) \in \mathbb{R}$ at lag τ as:

$$RMD(\tau) = \log_2 \left(\frac{1}{N'} \sum_{i=1}^{N'} RMD_i(\tau) \right), \tag{8}$$

where $N' = N - \tau$, and $RMD_i(\tau) = P(\mathbf{x}_i, \mathbf{y}_i(\tau))/(P(\mathbf{x}_i)P(\mathbf{y}_i(\tau)))$, if we consider Y to be shifted by τ units. For two independent systems X and $Y(\tau)$, $P(\mathbf{x}_i, \mathbf{y}_i(\tau)) = P(\mathbf{x}_i)P(\mathbf{y}_i(\tau))$, which implies that $RMD(\tau) = 0$. For $\tau > 0$, non-zero RMD implies that Y is dependent on X and the converse is true for $\tau < 0$. Note that RMD can quantify both uni- and bi-directional dependencies as well as multiple lags at which the systems might influence each other.

4 Testing for significance of observed values

In analyses of connectivity between pairs of experimental datasets, the measures used to quantify dynamical similarity often yield values that are intermediate, and we then cannot easily conclude whether the pair of time series are strongly or weakly connected. Even if we choose to define our measure so that it always lies within a finite interval – such as between 0 and 1 – experimental datasets can typically give ambiguous results of intermediate connectivity values such as 0.6. The connectivity measures obtained from such *passive experiments* cannot thus provide an unambiguous interpretation due to the lack of a comparative "test case". This is in contrast to *active experiments* (made, e.g., from laboratory experiments or numerical simulations of models) where the obtained values can be used for a consistent interpretation by its comparison to the uncoupled case. In passive experiments, the observed values of connectivity have to be statistically tested to ensure that they could not have been obtained by random chance. The statistical test is carried out using surrogate data sets generated from the observed time series in conjunction with an appropriate null hypothesis.

Surrogate time series are different from the original, observed ones, and yet preserve essential dynamical properties. There are several ways of generating surrogates and each method has its respective null hypothesis. The test statistic (which is RMD in our case) is calculated for a sufficiently high number of surrogate pairs and the observed value is tested for statistical significance using the obtained distribution and the appropriate null hypothesis.

For our analysis, we use a recurrence-based approach to generate *twin surrogates* (TS) from the observed time series [27,28]. *Twins* are two points $\mathbf{x}_i$ and $\mathbf{x}_j$ of X such that they share the same neighbourhood upto the limit ε, i.e., for $k = 1, 2, \ldots, N$, $\mathbf{R}^X_{k,i} = \mathbf{R}^X_{k,j}$. The TS method requires that we first identify all possible twins given an observed trajectory $\mathbf{x}$. To generate the surrogate series $\mathbf{s}$, we then choose an arbitrary random point $\mathbf{x}_k \in \mathbf{x}$ and set it as $\mathbf{s}_1$. Now, given $\mathbf{s}_i = \mathbf{x}_l$, we append subsequent points to $\mathbf{s}$ iteratively according to the following rule: when $\mathbf{x}_l$ has no twins, $\mathbf{s}_{i+1} = \mathbf{x}_{l+1}$; on the other hand when $\mathbf{x}_l \in T$ such that $T = \{\mathbf{x}_l\} \cup \{\mathbf{x}_m : \mathbf{x}_m$ and $\mathbf{x}_l$ are twins$\}$ and the number of elements in T is n, then $\mathbf{s}_{i+1} = \mathbf{x}_{k+1}$ where $\mathbf{x}_k \in T$ with probability $1/n$.

The null hypothesis for TS is that each surrogate trajectory is an independent realization of the system corresponding to a different initial condition. To test whether the observed value of $RMD(\tau)$, between X and $Y(\tau)$, is a statistically significant measure of X driving Y we do the following: (i) generate TS of Y, (ii) obtain a test distribution of $RMD(\tau)$ using the observed time series of X and the surrogates of Y, (iii) construct a 95% confidence band from the area between the 2.5^{th} and 97.5^{th} percentiles. This interval represents the region where we fail to reject the null hypothesis.

Observed values of RMD outside the confidence band imply a statistically significant dependence between X and Y at delay τ.

5 Method

The analysis is divided into two parallel components corresponding to the CRUTA and GISS temperature datasets. For each of these we consider delays of up to 150 months and estimate RMD, and test the observed values for significance. Similarly, we analyze all possible combinations for the forcing datasets as well as between the forcings and the temperature datasets. All results are grouped according to the "driven" dataset.

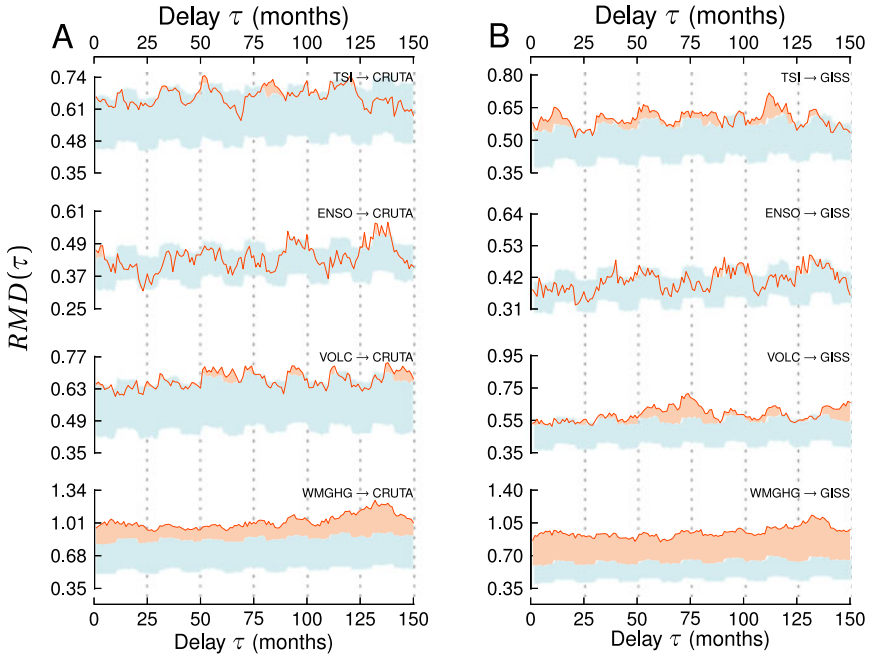

Fig. 2. Lagged influences on GMT. A. The results for the HadCRUT3v dataset. **B.** The results for the NASA GISS LOTI dataset. The 95% confidence band obtained from the significance test using TS is in **light blue**. The observed values of $RMD(\tau)$ is in **dark orange**. Regions where the value of $RMD(\tau)$ falls outside the confidence band are shaded in **apricot**. The datasets are labelled as mentioned in Sect. 2.

We do not embed the time series while constructing the recurrence matrices. Several recurrence properties are invariant under embedding and it is not essential to embed the time series. In particular, time delay embedding was not feasible for all of the datasets considered in this study and was hence avoided. The recurrence threshold was based on fixed amount of nearest neighbours, which was kept at 5% for all datasets. The qualitative nature of our results are robust to the choice of this threshold value because small changes in the threshold do not alter the qualitative features of the recurrence plot (result not shown).

The significance tests were carried out using 500 TS of the "driven" dataset. Significant values were then considered to construct an approximate network visualization of the dependencies involving the temperature dataset as well as the various radiative forcings.

6 Results and discussion

The results of the analysis for the temperature datasets are shown in Fig. 2, from which several points are initially evident.

– TSI appears to impact the GISS dataset more than it does the CRUTA data. In fact, even on short time scales of around a few months, the impact of TSI on CRUTA is barely significant. In previous studies by Lean & Rind [5,6] (done with the CRU data), TSI is found to influence variations in GMT on the scale of a month from their analysis based on multivariate regression.

- ENSO clearly has a sharp impact on the CRUTA series at a short delay of around 5 months (similar to Lean & Rind.). However, we also find further significant influences at delays of (approximately) 130 months for the CRU data, and at 90 months and 130 months for the GISS LOTI data. ENSO, however, does not have any impact on GISS temperatures at shorter time scales.
- Even though volcanic aerosols impact both temperature series on short time scales of around 1–10 months (Lean & Rind find 6 months), here too, there are further delayed interactions significant in the 50–75 month period and even as late as 140–150 months. This is discussed in more detail later.
- The influence of greenhouse gases on GMT is statistically significant for all values of delay considered and this influence peaks at around a delay of 130 months (approximately 11 years). This value is close to the previously considered value of 120 months in the Lean & Rind study.

The results of our analysis for the rest of the data are given in Fig. 3, grouped according to the "driven" dataset. The following points are discernible from Fig. 3.

- None of the datasets show a significant result when being tested against the hypothesis that they drive TSI (Fig. 3A). This demonstrates that, provided the datasets are accurate, our approach is able to rule out physically unreasonable connections.
- Both the temperature datasets seem to drive the ENSO time series at several values of τ (Fig. 3B). However, a noticeable dark band around the period of 25–30 months for both CRUTA and GISS suggest a strong influence of GMT on ENSO around the quasi-biennial oscillatory period. The reverse connection from ENSO to temperature has been discussed in earlier studies (cf. [30] and [31]). However, this feedback from the temperature to ENSO around the quasi-biennial period has not been considered in much detail and thus needs more careful investigation. The greenhouse gases too seem to impact ENSO in around this period. The greenhouse gas series also impacts ENSO around 55–60 month period which might be linked to a quasi-quadrennial kind of phenomenon [32]. Similar influence of greenhouse gas emissions on the ENSO have been discussed elsewhere [33,34].
- Only TSI and ENSO seem to have an effect on the volcanic activity dataset (Fig. 3C) with the former influencing VOLC at a short time scale of around 1–5 months and the latter influencing it rather strongly at around 30 months. The idea that climatic phenomena could influence volcanic activity is controversial and debatable (e.g., [35] postulates one possible mechanism based on lithospheric stress). However, [36] challenges the more popular idea that ENSO is influenced by volcanic eruptions and suggests a converse dependency, with one possible physical mechanism being the influence of oceanic angular momentum on the earth's rotation rate at subdecadal scales (cf. Marcus et al. [37]) which in turn might influence seismic activity on the mantle. Alternatively, the transport of volcanic aerosols in the atmosphere could be influenced as well which might lead to the results observed here (also discussed below). Our results indicate that it might be worthwhile to study this more closely in order to gain a better understanding of globally relevant climatic phenomena such as volcanoes and the ENSO.
- The greenhouse data is influenced by only the TSI and the VOLC datasets (Fig. 3D) at similar values of τ around 50–55 months. The impact of VOLC on the greenhouse gases most likely reflects the response of the Earth's carbon-cycle to volcanic eruptions (e.g., [38]). The observed influence of TSI on WMGHG could be an example of indirect influence of TSI on the WMGHG data via the VOLC dataset as the TSI impacts VOLC at much shorter time scales of a few months.

The above results are summarized as a network of dependencies in Fig. 4, where two different directed networks are visualized: one each for the two temperature datasets

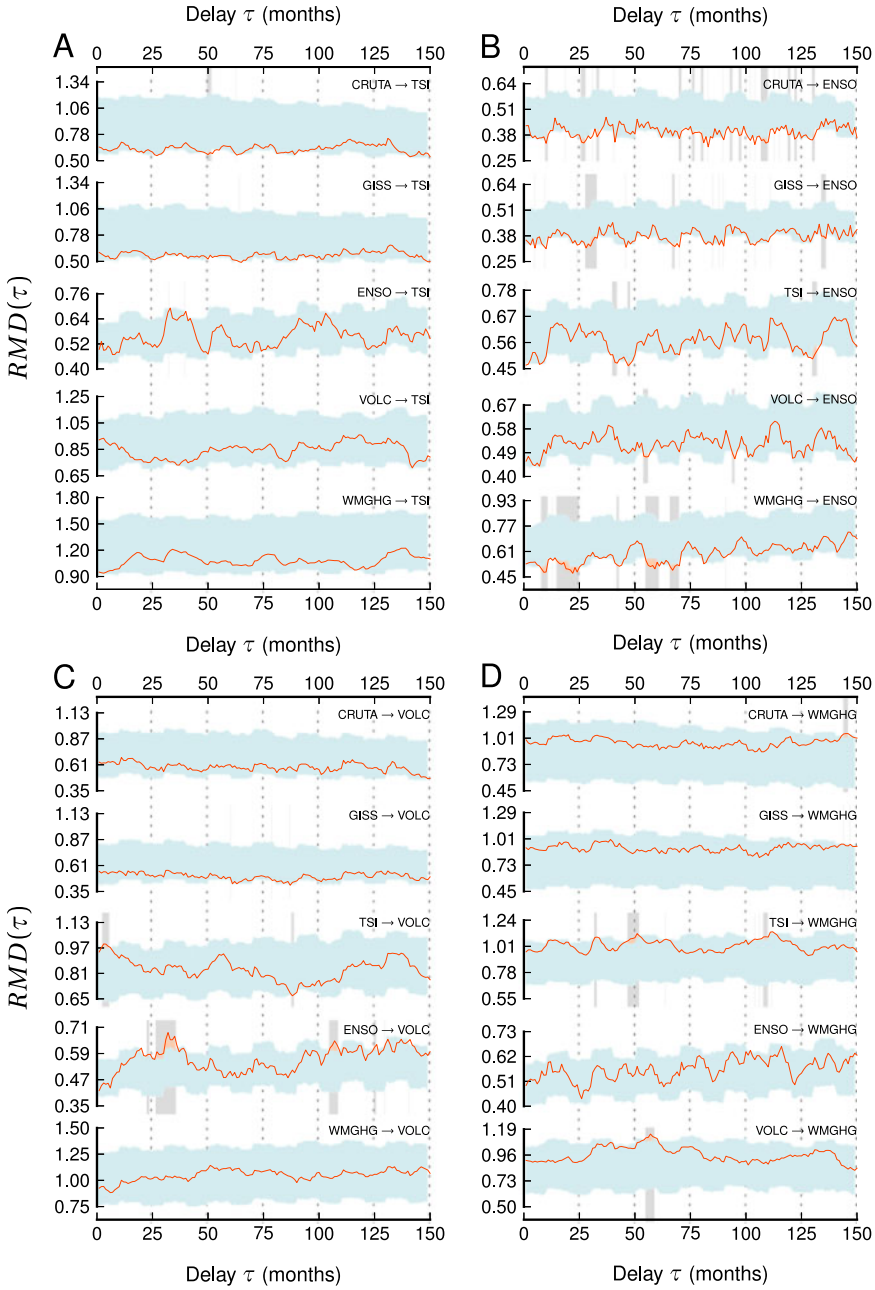

Fig. 3. Lagged dependencies among the forcing datasets. A. Results for the other datasets driving TSI. **B.** Results for the other datasets driving ENSO. **C.** Results for the VOLC dataset being driven by the others. **D.** Results for the WMGHG dataset being driven by the rest. Legends and keys to the figure are same as in Fig. 2. The grey bars highlight the values of τ for which the observed values of RMD are statistically significant.

– CRUTA and GISS. Only statistically significant values are used to construct these networks. However, from Fig. 2 and Fig. 3, we see that, in many cases, there are multiple values of τ at which estimated values of RMD are significant for a given pair of datasets. In such cases, for the sake of visual clarity, a single value of τ is

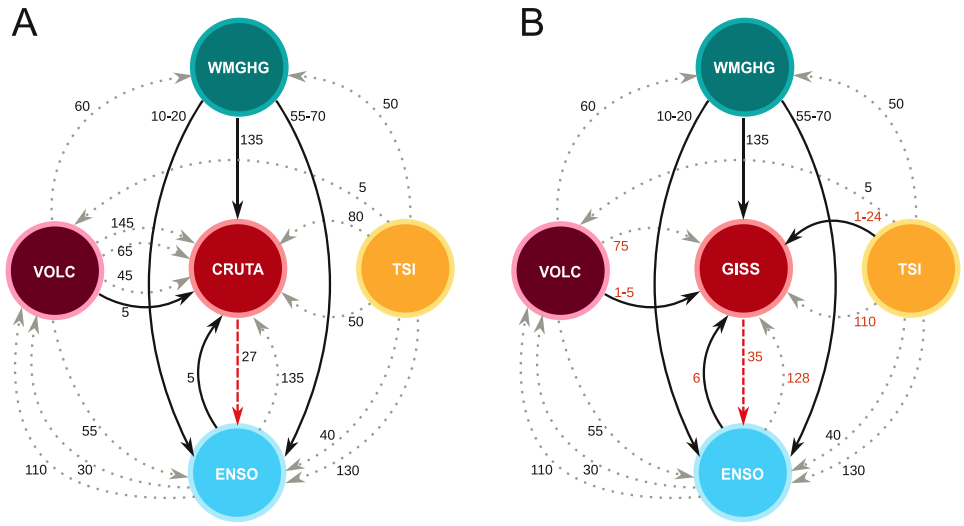

Fig. 4. Network of dependencies surrounding GMT. A. For the HadCRUT3v temperature series. **B.** For the NASA GISS LOTI series. The arrows correspond to a statistically significant influence. The numbers beside the arrows denote the (interval of) delay(s) at which the statistically significant link is found. In **B**, the τ values that differ from **A** are given in red. The solid black arrows correspond to links that are known and/or are discussed to some extent in the literature. The gray dotted arrows correspond to links that are not easily explained. The red dashed arrow is the feedback from temperature to ENSO that is uncovered by our analysis. The datasets are labelled as given in Sect. 2: *CRUTA* for the HadCRUT3v data; *GISS* for NASA GISS LOTI; *TSI* for total solar irradiance; *VOLC* for the optical aerosol depth data; and *WMGHG* for the well-mixed greenhouse gas series. *Note*: For the links between WMGHG and temperature, and TSI and temperature, only a few of the statistically significant values are shown for visual clarity.

chosen as representative of (nearly) continuous intervals of τ in which RMD values are significant. In case the interval is too wide for a single value to be representative, the interval itself is mentioned. Two notable exceptions to this are the links between WMGHG and CRUTA/GISS, and TSI and GISS. In these cases, RMD values are significant for almost all values of τ considered – and hence only the presumably physically relevant values of τ are shown in Fig. 4 for clarity. We choose here $\tau = 135$ months as this is the peak value of $RMD(\tau)$ for these pairs and is also close to the earlier estimated value of $\tau = 120$ months in [5]. We note that the networks shown in Fig. 4 are not constructed on the basis of a mathematical procedure. They are, in fact, intended to reveal the *qualitative* structure of the network of interactions among global temperature drivers. We can infer the following from Fig. 4:

- The results for the CRUTA and GISS temperature datasets are reasonably consistent for the links with ENSO, WMGHG and VOLC, but differ in the case of their respective links with TSI.
- TSI seems to drive all the remaining four datasets. However, the delays at which TSI impacts them are much larger than what is normally assumed in studies involving TSI and GMT. Our results indicate that it might be possible that the longer time scale periodicities of solar irradiance might be an important factor influencing global climatic phenomena.
- The GMT feeds back into *only* the ENSO series near the quasibiennial period (the results are slightly different between CRUTA and GISS here). This might be a

crucial point to consider in both (semi-) empirical as well as theoretical modeling of GMT in terms of natural forcings.
- Apart from having a distinctively significant impact on the GMT, greenhouse gases influence the ENSO as well at multiple delays. Two distinctive periods in which WMGHG drives the ENSO are around 1–2 years and 4–6 years.
- Volcanic aerosols seem to impact GMT not only at the evident short time scales of a few months, but also at other time scales ranging from 45 months to 145 months, which is relatively hard to justify considering that volcanic aerosols do not last in the atmosphere up to 145 months. This example demonstrates the limitations of our approach and is discussed below.

One obvious limitation of our approach is the uncertainty of the statistical test itself. Thus, even when we find a link to be significant (with respect to the previously stated null hypothesis) at a 5% level of significance, we could be wrong 5 times out of 100. A second limitation, and one that might cause, e.g., the suspicious result of VOLC impacting GMT at 145 months, is that the 'volcanic activity' is represented here by the optical depth of stratospheric aerosols. This quantity, in time periods located away from major volcanic eruptions, might be influenced by the other climatic factors. However, a third, and more critical limitation is that our approach cannot distinguish indirect/spurious links from direct ones. This means that if we have: (i) X drives A and A drives Y, or (ii) A drives both X and Y, in both cases our method would show a link between X and Y even though there is no direct connection between them. The direction of this link might then be influenced by random noise (if any) in the systems. We feel that the impact of volcanic aerosols on the GMT at delays as large as 145 months might most likely be due to spurious links that are not removed. There are other methods, e.g., multivariate transfer entropy [39], which can detect and remove spurious links. It is computationally intensive and difficult to incorporate such a principle into the current recurrence-based approach and is thus intended as a goal of future investigations.

7 Conclusion and outlook

We present a recurrence-based approach to investigate the network of dependencies among the various factors that are known to influence global mean temperature. To the best of our knowledge, this is a first attempt to consider various climatic factors, such as the ENSO, volcanic activity, greenhouse gas concentration, and solar irradiance, as nodes of an interacting, directed network. To construct the network, we extend the notion of an existing recurrence-based connectivity measure and propose a new, general measure that detects the level of probabilistic dependence between two datasets based on their joint recurrences. The study also illustrates the use of twin surrogates as a suitable tool for surrogate-based hypothesis testing, crucial for the interpretation of measures estimated from passive experiments.

Our analysis uncovers an intricate, directed network with multiple edges between the nodes.We find a feedback from global temperature to ENSO around the quasi-biennial period, and also significant influences between ENSO and volcanic aerosols – both of which issues require further understanding and investigations. The results indicate the need to consider additional interactions (and at different delays) among the climatic factors considered in order to formulate a more complete picture of global mean temperature variations. This is crucial for the purpose of foreseeing future variations in the temperature. We intend the results to serve as indicators for both (semi-) empirical as well as well theoretical models of global mean temperature.

This study illustrates a new way of investigating climatic phenomena as networks, a view which can be extended, e.g., by including additional factors (such as

stratospheric water levels, ozone concentrations, snow albedo, etc.) related to global mean temperature. Investigation of these connections using paleoclimatic datasets can give us further insight on the evolution of global temperature. The datasets considered here can be further considered as networks themselves – where the nodes could be geographical grid points, or sub-factors from which the data were constructed – leading to an interacting network of networks [40] involving the global mean temperature.

This study was financially supported by the DFG research group HIMPAC (FOR 1380), the German Federal Ministry of Education and Research (BMBF project PROGRESS, 03IS2191B) and the EU 7th Framework Program under a Marie Curie ITN, project LINC. The authors wish to thank Judith Lean for providing electronic data.

Appendix

A Data sources

The datasets used in this analysis are available (as of December 1, 2012) for download at the web addresses listed below.

- Multivariate ENSO Index
  - From 1950 to present
    `http://www.esrl.noaa.gov/psd/enso/mei/table.html`
  - Prior to 1950
    `ftp://www.coaps.fsu.edu/pub/JMA_SST_Index/`
- Stratospheric optical aerosol depth
  `http://data.giss.nasa.gov/modelforce/strataer/tau_line.txt`
- Total Solar Irradiance
  `http://lasp.colorado.edu/sorce/tsi_data/TSI_TIM_Reconstruction.txt`
- WMGHG forcing
  `http://data.giss.nasa.gov/modelforce/RadF.txt`
- NASA GISS LOTI
  `http://data.giss.nasa.gov/gistemp/tabledata_v3/GLB.Ts+dSST.txt`
- HadCRUT3v global mean temperature
  `http://www.cru.uea.ac.uk/cru/data/temperature/hadcrut3v.zip`

References

1. G.C. Hegerl, et al., *Climate Change 2007: The Physical Science Basis. Contribution of Working Group I the Fourth Assessment Report of the Intergovernmental Panel on Climate Change*, Vol. 9 (Cambridge Univ. Press, Cambridge, UK 2007), p. 663
2. K.E. Trenberth, et al., *Climate Change 2007: The Physical Science Basis. Contribution of Working Group I the Fourth Assessment Report of the Intergovernmental Panel on Climate Change*, Vol. 3 (Cambridge Univ. Press, Cambridge, UK 2007), p. 663
3. J. Hansen, R. Ruedy, M. Sato, K. Lo, Rev. Geophys. **48**, RG4004 (2010)
4. R.E. Benestad, Environ. Res. Lett. **7**, 011002 (2012)
5. J.L. Lean, D.H. Rind, Geophys. Res. Lett. **35**, L18701 (2008)
6. J.L. Lean, D.H. Rind, Geophys. Res. Lett. **36**, L15708 (2009)
7. G. Foster, S. Rahmstorf, Environ. Res. Lett. **6**, 044022 (2011)
8. N. Marwan, Eur. Phys. J. Special Topics **164**, 3 (2008)
9. J.P. Zbilut, N. Thomasson, C.L. Webber, Med. Eng. Phys. **24**, 53 (2002)
10. J.A. Bastos, J. Caiado, Phys. A **390**, 1315 (2011)
11. J. Serrà, X. Serra, R.G. Andrzejak, New J. Phys. **11**, 093017 (2009)

12. D.C. Richardson, R. Dale, Cognitive Sci. **29**, 1045 (2005)
13. N. Marwan, M.H. Trauth, M. Vuille, J. Kurths, Clim. Dyn. **21**, 317 (2003)
14. S. Li, Z. Zhao, Y. Wang, Y. Wang, Environ. Earth Sci. **64**, 851 (2011)
15. M.C. Romano, M. Thiel, J. Kurths, I.Z. Kiss, J.L. Hudson, Europhys. Lett. **71**, 466 (2005)
16. K. Walter, M.S. Timlin, Weather **53**, 315 (1998)
17. S.D. Meyers, J.J. O'Brien, E. Thelin, Mon. Weather Rev. **127**, 1599 (1999)
18. M. Sato, J.E. Hansen, M.P. McCormick, J.B. Pollack, J. Geophys. Res. **98**, 987 (1993)
19. Y.-M. Wang, J.L. Lean, N.R. Sheeley, Jr., Astrophys. J. **625**, 522 (2005)
20. J. Hansen, et al., Clim. Dyn. **29**, 661 (2007)
21. P. Brohan, J.J. Kennedy, I. Harris, S.F.B. Tett, P.D. Jones, J. Geophys. Res. **111**, D12106 (2006)
22. J.-P. Eckmann, S.O. Kamphorst, D. Ruelle, Europhys. Lett. **4**, 973 (1987)
23. N. Marwan, M.C. Romano, M. Thiel, J. Kurths, Phys. Rep. **438**, 237 (2007)
24. M.C. Romano, M. Thiel, J. Kurths, C. Grebogi, Phys. Rev. E **76**, 036211 (2007)
25. Y. Zou, M.C. Romano, M. Thiel, N. Marwan, J. Kurths, Int. J. Bifurcat. Chaos **21**, 1099 (2011)
26. N. Marwan, Y. Zou, N. Wessel, M. Riedl, J. Kurths, Proc. R. Soc. A (submitted) (2012)
27. M. Thiel, M.C. Romano, J. Kurths, M. Rolfs, R. Kliegl, Europhys. Lett. **75**, 535 (2006)
28. M. Thiel, M.C. Romano, J. Kurths, M. Rolfs, R. Kliegl, Phil. Trans. R. Soc. A **366**, 545 (2008)
29. O. Miettinen, J. Wang, Am. J. Epidemiol. **114**, 144 (1981)
30. M. Ghil, R. Vautard, Nature **350**, 324 (1991)
31. V. Moron, R. Vautard, M. Ghil, Clim. Dyn. **14**, 545 (1998)
32. N. Jiang, J.D. Neelin, M. Ghil, Clim. Dyn. **12**, 101 (1995)
33. S.L. Stevenson, Geophys. Res. Lett. **39**, L17703 (2012)
34. S. Stevenson, B. Fox-Kemper, M. Jochum, R. Neale, C. Deser, G. Meehl, J. Clim. **25**, 2129 (2012)
35. M.R. Rampino, Science **206**, 826 (1979)
36. A. Robock, Rev. Geophys. **38**, 191 (2000)
37. S.L. Marcus, Y. Chao, J.O. Dickey, P. Gegout, Science **281**, 1656 (1998)
38. C.D. Jones, P.M. Cox, Global Biogeochem. Cycles **15**, 453 (2001)
39. J. Runge, J. Heitzig, V. Petoukhov, J. Kurths, Phys. Res. Lett. **108**, 258701 (2012)
40. J.F. Donges, H.C.H. Schultz, N. Marwan, Y. Zou, J. Kurths, Eur. Phys. J. B **84**, 635 (2011)